

Power Quality Analysis Using An Adaptive Decomposition Structure

Doğan Gökhan Ece¹ and Ömer Nezh Gerek¹

(1) Dept. of Electrical and Electronics Engineering, Anadolu University, School of Engineering and Architecture, Eskisehir 26470, Turkey (e-mail: dgece@anadolu.edu.tr, ongerrek@anadolu.edu.tr)

Abstract – A new event detection scheme for power quality analysis based on the statistical analysis of adaptive decomposition signals is proposed. Proposed scheme is implemented using MATLAB™ Simulink DSP Blockset. The combination of an adaptive prediction filter based subband decomposition structure with a rule based histogram analysis block produced successful detection and classification results on our real life power system transient data.

Keywords – Power quality analysis, Statistical methods, Adaptive decomposition.

I. INTRODUCTION

Event detection and classification are essential processes for explaining and then correcting the cause of the power quality (PQ) problems in low-voltage, commercial, and industrial applications. Once the voltage and/or current waveforms are captured and stored, an automated post event analysis is needed. Considering the range of equipment operated on the customer's side of the meter, the analysis tool should be immune to the inherent noisy and harmonically rich normal operating conditions while adapting to the dynamic changes in customer's load to avoid nuisance alarm signals. Recent contributions in the area of PQ analysis use various wavelets such as Daubechies wavelets, Morlet wavelets, etc., to analyze the disturbances while pre-event voltage or current waveforms are assumed to be sinusoid [5]-[9]. A specific wavelet may be designed to detect, for example, arcing faults in a sinusoidal pre-fault waveform [10]. However, the selected wavelet may not correspond to the optimal discriminating system for another type of a transient event.

In this work, a new event detection scheme for power quality analysis based on the statistical analysis of adaptive decomposition signals is proposed. The adaptive method is developed to detect and classify power quality disturbances regardless of the type of the pre-event voltage or current waveforms. The significance of the proposed method is that it provides a way of detecting variety of events without changing the structure.

If we do not have any prior information on whether the waveform is pure sinusoid, or not, the steady state properties of a waveform can be well approximated using adaptive systems. The only assumption is that the pre-event steady state waveform has variations of relatively lower frequency as compared to the noise imposed waveform due to a transient event. This idea is utilized to construct a

decomposition filter bank structure [1] which operates on the current or voltage waveforms, and at the same time, adapts its filter bank according to the waveform behavior. Least Mean Squared (LMS) type adaptive filters are used in our filter bank structure [3]. These filters are time-varying FIR filters whose coefficients are continuously updated according to the minimization of an error sequence, which corresponds to one of the subbands in our case. When the adaptation converges to a steady state, the disturbance contribution of any transient event on the waveform will take some time for the adaptive filter bank to adapt. Meanwhile, the decomposition structure will exhibit large adaptation error signals in the high-pass subband. Time length of this large adaptation error signal is expected to be short for transient-type events such as arcing line-to-ground faults, sags, and swells and the adaptation time is expected to be longer for dynamic changes in load. The theoretical background of the statistical properties of this structure is explained in detail in [1].

This method is also able to detect changes in the nature of any kind of steady state waveforms. Theoretically, if the steady state waveform has high frequencies, and if the disturbance causes low frequency components, the adaptation will again be perturbed producing large adaptation errors. However, success for this case is limited by the ability of convergence speed of the adaptation algorithm (LMS). A general case of relatively lower frequency steady state waveforms generated under normal operating conditions, as compared to higher frequency components generated by PQ events can be safely assumed for the majority of applications.

For our tests, real life voltage and current data are obtained from a low-voltage experimental system during various type of staged transient events. Proposed method is implemented using MATLAB™ Simulink DSP Blockset [11]. During the detection process, the event data is applied to the system which is a combination of an adaptive prediction filter based subband decomposition structure and a rule based histogram analysis block. In our experiments, we have observed that staged arcing faults, sag, and swell events can be detected, localized in time, and discriminated using this method. The ability to classify and distinguish transients from changes in load makes the proposed method more flexible as compared to the commonly used transform domain thresholding techniques for the analysis of power quality events.

II FILTERBANK STRUCTURE

The signal decomposition consists of an adaptive prediction filter in a polyphase structure [1]. In this aspect, the overall scheme resembles the lifting-style wavelet decomposition due to its filterbank implementation [2]. However, the basic idea is to produce decomposition signals which converge to a minimal residual signal that can be considered as the *non-predictable* content of the steady state signal. This idea is also very new in the signal processing field, and quite recently it has been applied to signal compression [1]. Normally, the wavelet filterbanks decompose the signal according to the frequency content of the filters with fixed coefficients. Here, the frequency content or spectral decompositions are irrelevant due to the fact that the adaptive prediction filter constantly changes the filter coefficients. Instead of a spectral decomposition, we split the signal into

- a) *lower resolution*, and
- b) *non-predictable* portions.

The analysis structure is illustrated in Fig. 1. Both the lower resolution and non-predictable parts are produced using the two polyphase components of the original signal:

$$x_1[n] = x[2n] \quad (1)$$

$$x_2[n] = x[2n+1] \quad (2)$$

These components can be thought of as even and odd indexed terms of the discrete-time signal. For a signal with slow variations, the two polyphase components have strong correlation. Therefore one of the polyphase components, let's say $x_2[n]$, can be successfully approximated using the other component samples $x_1[n]$ and a prediction filter, say, $P_1(\cdot)$. In that case, one can expect the difference between the prediction output and $x_2[n]$ to be relatively small:

$$\varepsilon = x_2[n] - P_1(x_1[n-m], \dots, x_1[n-m])$$

Comparing the above difference with Figure 1, it can be seen that the difference sequence corresponds to the lower branch output: $x_h[n]$.

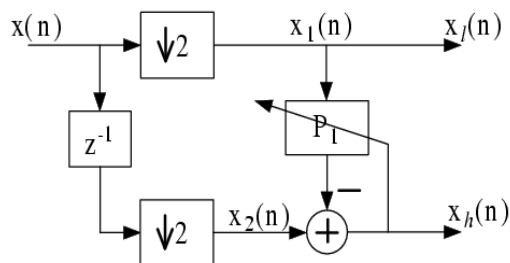


Fig. 1 Analysis stage of the 2-channel adaptive filter bank

LMS adaptation attempts to obtain the optimum (in the mean-squared sense) prediction filter by updating the filter coefficients according to the minimization of the error se-

quence, $x_h[n]$. The LMS update is a straightforward operation for adaptive predictive filtering, and can be found in any kind of literature which deals with adaptive processes [3], [4]. However, the use of LMS adaptation inside a polyphase decomposition structure is a new approach [1]. Notice that conventional adaptive predictive filtering uses a causal prediction stage. By using polyphase components, the adaptive prediction becomes non-causal, improving the inter-correlation of the samples. In [1], theoretical details are provided, and it has been shown that this structure statistically minimizes the error signal energy of the polyphase components for a steady state signal. We have adopted this new adaptive decomposition approach for the analysis of power system waveforms due to its ability to produce low-magnitude signals while the input is steady, and to produce high-magnitude portions when the steady characteristics of the input waveform is disturbed.

A. Simulink implementation of the adaptive filterbank

A commonly used tool for automated post processing of signals is MATLAB™ Simulink. The built in functions and blocksets, together with the visual programming environment make Simulink a preferable tool. We developed an integrated detection tool using DSP blocksets. The adaptive filterbank portion of the integrated layout is shown in the dashed portion at the left of Figure 2. This portion can be easily matched to the structure shown in Figure 1. Notice that the signal is first decomposed into polyphase components by downsampler and integer delay modules. The above polyphase component, $x_1[n]$, is directly fed into the LMS block as the input signal. The other component, $x_2[n]$, is delayed by a factor of 10, which is half of the filter tap size of the LMS block, and compared to the LMS output using a subtraction module. The result of this difference corresponds to $x_h[n]$ and it is fed back to the error input part of the LMS block, by which the adaptation occurs. The rest of the Simulink layout deals with the analysis of the produced $x_h[n]$.

III STATISTICAL ANALYSIS

The residual output, $x_h[n]$, generated by the adaptive decomposition block carries clearly visible information about the detection of various types of events. Therefore, it may be sufficient to present the above decomposition which produces necessary features for detection, and leave the detection part to the practicing engineer. Nevertheless, we give a sample detection method to post-process the adaptive decomposition output with satisfactory results. In this work, we developed an experimental histogram-based analysis stage which provides automated detection. The analysis stage consists of a windowed-histogram generation block and the statistical analysis of the histogram. Statistically, the windowed-histogram provides a short-time approximation of the density function, *pdf*. The *pdf*

naturally carries all the statistical information of a process, therefore its approximation, the histogram, is also observed to be useful for generating the detection rule.

In the adaptive decomposition structure explanations, we have seen that the residual error $x_h[n]$ becomes large in magnitude when an event happens. This is clearly the point that must be detected. If we monitor $x_h[n]$ signal in a time-windowed manner, we can see that the histogram is

well centered when the magnitudes of $x_h[n]$ samples are small. This is the case when the waveform exhibits no event. As soon as an event happens, due to large-in-magnitude samples of $x_h[n]$, its histogram becomes no longer centered. Instead, the tails of the histogram becomes heavy. An example for this case is given in Figure 3.

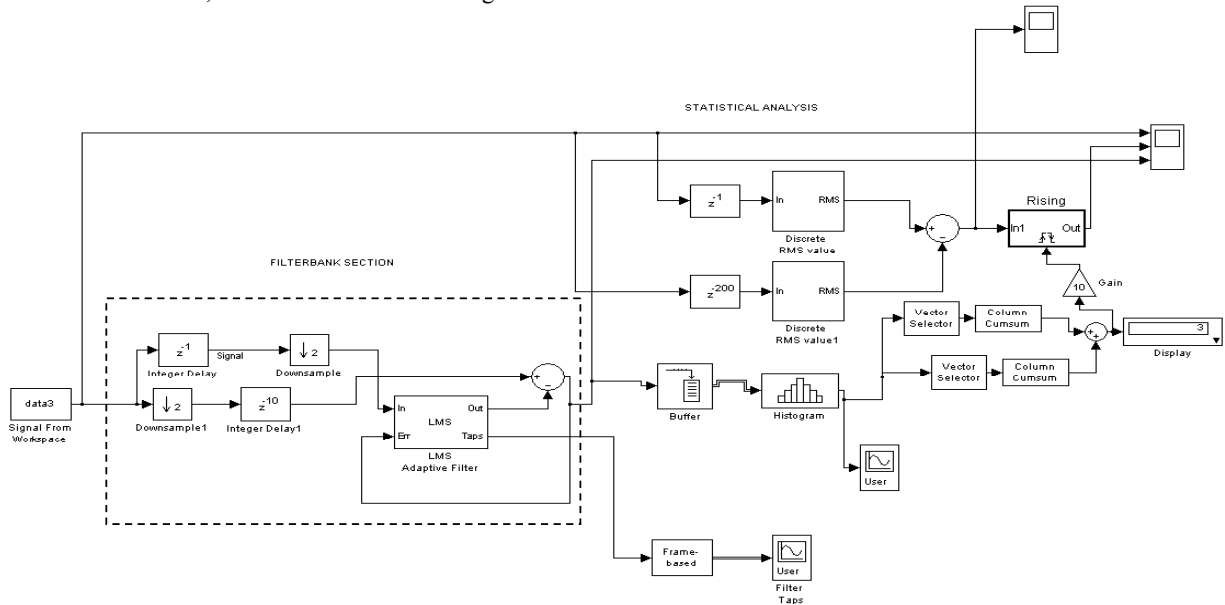


Fig. 2: Simulink layout of the system.

Using the above observation, we developed a simple comparison rule in which we compare the weight of the center and tail portions of the histogram. If the tails are weak as compared to the center portion, it means there is no event. If the tails are heavy, then we trigger an event alarm.

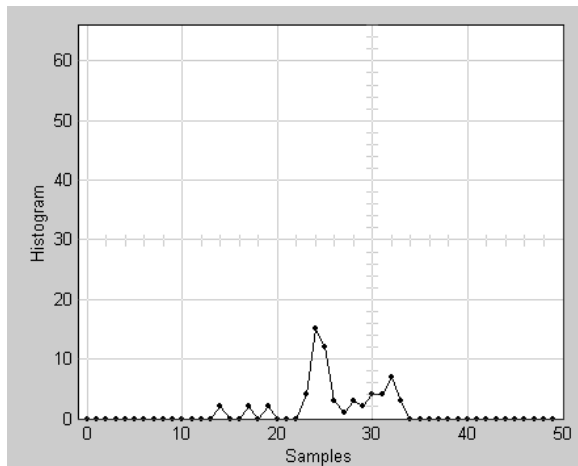


Fig. 2: Example histogram during event.

A. Simulink implementation of the statistical analysis

Similar to the previous case, we implemented the statistical analysis using Simulink. Inside the integrated layout, the statistical analysis portion corresponds to the bottom-right portion of Figure 2.

The $x_h[n]$ signal is first buffered to produce a time-windowed portion. Then this vector is fed into a component which calculates the histogram. Next, two vectors, corresponding to two portions of the histogram are extracted from the histogram using the vector selector blocks. These portions are the central and the tail portions. The weight of these two vectors are then calculated and compared. The output of the comparison is the immediate point of detection of an event.

There are other blocks in the integrated system which are activated by the event. These blocks are designed to discriminate arcing faults from sags and swells. RMS changes in the waveform before and after the event triggered calculating blocks shows that arcing fault type events triggers the system frequently during the event. Therefore the RMS comparisons are performed frequently, and the comparator output produces bursts of noisy shapes. On the other hand, sags and swells trigger the detection block more uniformly. The difference between a sag and a swell is determined by the direction of the comparator output. Detailed explanations of this portion together with real life demonstrations

are presented in the experimental results.

IV EXPERIMENTAL RESULTS

Experimental system is composed of a three-phase, 380 V, 50 Hz, 5-wire supply loaded with RL load banks and three-phase induction motors coupled with varying mechanical loads. System also enables the use of adjustable speed drives to control the induction motors when required. Transient events used for testing the proposed method are phase-to-ground arcing fault, voltage sag due to an induction motor starting, and momentary change in load. While line-to-line voltages of the experimental system were sampled for the first two types of events, phase currents were sampled for the last type.

A line-to-ground arcing fault event data is applied to the Simulink implementation of the proposed system and the

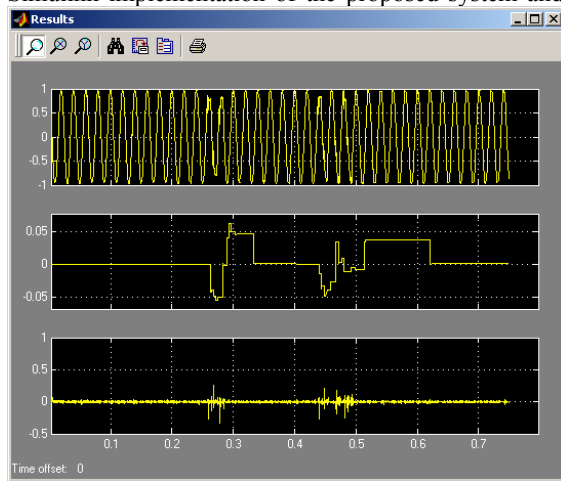


Fig. 4 Arcing Fault (Top: faulted line-to-line voltage waveform, Middle: Change in the rms value of the voltage, Bottom: Adaptation error signal)

output is illustrated in Figure 4. Although we staged a line-to-ground fault, the faulted line-to-line voltage waveform, that is effected from the fault more, is considered due to the fact that the ground path may not always be reachable from the location of a digital event recorder in a real life system. Fault first starts around 0.25 second and strikes again after extinguishing for several cycles. This is also perfectly visible in the adaptation error signal which is fed in to the statistical analysis block to trigger the digital RMS voltage measurement block. As expected, some amount of voltage collapse is observed during the fault besides the additive noise due to the nature of arcing fault. Although the primary event here is an arcing fault, this reduction in the voltage magnitude corresponds to a sag event, too. After the fault extinguishes and the system voltage returns to normal, then the event corresponds to a swell event. Middle waveform in Figure 4 shows the change in the RMS value of the voltage in successive periods. With the fault present, as the adaptation error yields large random bursts, a drop in RMS value with noisy steps

are observed. In contrast, as the fault recovers, a rise in RMS value again with noisy steps are observed. Note that these noisy steps are due to the nature of the arcing fault. Finally, the system voltage recovers completely and the change in RMS value of the system voltage becomes zero following the adaptation to the new state.

A voltage sag event due to an induction motor starting is illustrated in Fig. 5. Significant reduction in voltage waveform is observed. Detection of any type of event using an adaptive decomposition scheme, wavelet transformation, and other frequency domain techniques would become easier if there is some high frequency noise at the start of an event. However, as shown in Figure 5, voltage variation during the sag event is very smooth and free of noise. Even in this case, there is a large adaptation

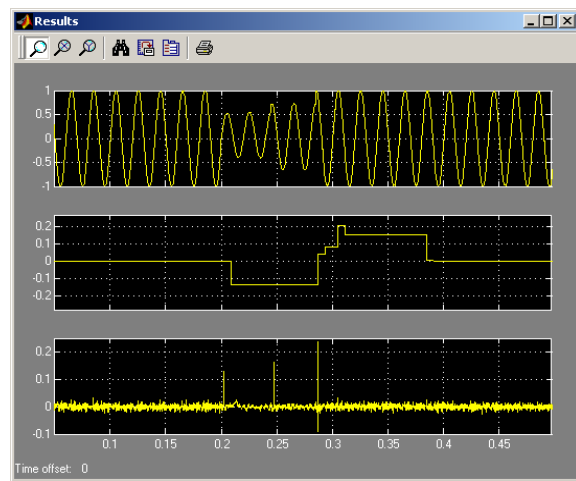


Fig. 5 Voltage sag event (Top: line-to-line voltage waveform, Middle: Change in the rms value of the voltage, Bottom: Adaptation error signal)

error which triggers the RMS voltage measurement block and a sharp drop of RMS voltage magnitude is seen as given in the middle waveform of Figure 5. This sharp drop of RMS magnitude of the voltage should be compared with the reduction with noisy steps as observed in arcing fault case given in Figure 4. For the voltage sag, reduction in the RMS voltage is larger than that of arcing fault. In addition, the duration of voltage sag due to a motor starting is longer than that of arcing fault. When the motor reaches its nominal speed, the system voltage recovers and a few cycles later adaptation to the state prior to sag event is restored again. In this case the adaptation time is longer than that of the arcing fault due to the fact that the variation in the RMS voltage is larger and the filterbank requires more time to adapt. Towards the end of the sag event, some load injected noise is overimposed on the voltage waveform causing a step like increase to its original RMS value. This step like increase is also very different than the noisy steps shown in arcing fault case.

Monitoring the phase currents is also possible using the proposed scheme. A phase current of the experimental

system during a momentary change in load configuration is shown in Fig. 6. Increasing change in the RMS value of the current during successive cycles indicates that an additional load is switched on. For an effective detection and discrimination of power quality events, both voltage and current waveforms should be monitored simultaneously. For example, non-linear loads such as adjustable speed drives distort system voltage by causing notching. Without monitoring the system current as well, it is difficult to conclude the source of this distortion. Although it causes a voltage sag event, induction motor starting is a normal event. System current information is also required to distinguish the cause of a voltage sag due to a motor starting or a short circuit. Note that if the waveform shown in Fig. 6 were a voltage waveform, the variation would be a swell event and it would be detected as such. In this case, increase in the

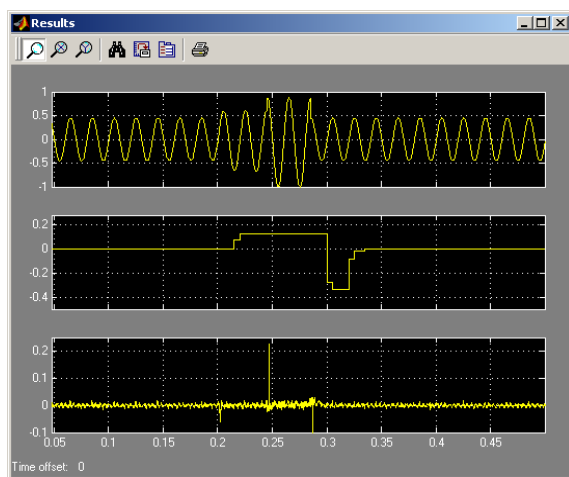


Fig. 6 Momentary change in load (Top: line current waveform, Middle: Change in the RMS value of the current, Bottom: Adaptation error signal)

RMS value of the voltage is larger than that of arcing fault case. In addition, the duration of the swell event is longer than the arcing fault event.

VI. CONCLUSIONS

Our experimental results indicate that histogram based analysis of the adaptive decomposition outputs can clearly distinguish events such as faults and abrupt changes from the steady state waveforms. The adaptive decomposition portions feeds the adaptation error sequence to a time-windowed histogram generating block. The central and tail histogram portions are then fed into comparators for an event detection. Once this statistical analysis portion detects an event, RMS measurement blocks are triggered and local RMS values before and after the trigger time are compared. By applying proper thresholds for the final comparator output, power quality events can be classified and dynamic changes in load can be distinguished.

ACKNOWLEDGMENTS

This work is supported by Anadolu University Research Foundation under Contract: 000212.

REFERENCES

- [1] O. N. Gerek and A. E. Cetin, "Adaptive Polyphase Subband Decomposition Structure for Image Compression," *IEEE Trans., Image Processing*, Vol. 9 (10), pp. 388-398, 2000.
- [2] I. Daubechies and W. Sweldens, "Factoring wavelet transforms into lifting steps," *J. Fourier Anal. Applicat.*, Vol. 4(3), pp. 247-269, 1998.
- [3] Simon Haykin, "Adaptive Filter Theory," Englewood Cliffs, NJ, Prentice Hall, 1986.
- [4] O. Arikan, A. E. Cetin, and Engin Erzin, "Adaptive Filtering for non-Gaussian Stable Process," *IEEE Signal Processing Letters*, Vol. 1(11), pp. 163-165, 1994.
- [5] S. J. Huang, C. T. Hsieh, and C. L. Huang, "Application of Morlet Wavelets to Supervise Power System Disturbances," *IEEE Trans. Power Delivery*, Vol. 14(1), pp. 253-243, 1999.
- [6] S. J. Huang and C. T. Hsieh, "High-Impedance Fault Detection Utilizing Morlet Wavelet Transform Approach," *IEEE Trans. Power Delivery*, Vol. 14(4), pp. 1401-1410, 1999.
- [7] A. M. Gaouda, M. A. Salama, M. R. Sultan, and A. Y. Chikhani, "Power Quality Detection and Classification Using Wavelet-Multiresolution Signal Decomposition," *IEEE Trans. Power Delivery*, Vol. 14(4), pp. 1469-1476, 1999.
- [8] Surya Santoso, W. Mack Grady, Edward J. Powers, J. Lamoree, and S. C. Bhatt, "Characterization of Distribution Power Quality Events with Fourier and Wavelet Transforms," *IEEE Trans. Power Delivery*, Vol. 15(1), pp. 247-254, 2000.
- [9] L. Angrisani, Pasquale Daponte, and M. D' Apuzzo, "Wavelet Network-Based Detection and Classification of Transients," *IEEE Trans. Inst. Measurement*, Vol. 50(5), pp. 1425-1435, 2001.
- [10] A. H. Tewfik, D. Sinha, and C. Jorgensen, "On the Optimal Choice of a Wavelet for Signal Representation," *IEEE Trans. Information Theory*, Vol. 38(2), pp. 747-765, 1992.
- [11] MATLAB Simulink, Natick, MA, The Mathworks, Inc.